Effects of Micro/Nano-Scale Surface Characteristics on the Leidenfrost Point Temperature of Water

Citation: Kim, Hyungdae et al. "Effects of Micro/Nano-Scale Surface Characteristics on the Leidenfrost Point Temperature of Water." Journal of Thermal Science and Technology 7.3 (2012): 453–462.

As Published: http://dx.doi.org/10.1299/jtst.7.453

Publisher: Japan Society of Mechanical Engineers, The

Persistent URL: http://hdl.handle.net/1721.1/84051

Version: Author's final manuscript: final author's manuscript post peer review, without publisher's formatting or copy editing

Journal of Template

Vol. 00, No. 0, 0000

Effects of micro/nano-scale surface characteristics on the Leidenfrost point temperature of water*

Hyungdae KIM**,*** Bao TRUONG*** Jacopo BUONGIORNO*** and Lin-Wen HU****

**Nuclear Engineering Department, Kyung Hee University
Youngin, Gyeonggi 446-701, Republic of Korea
E-mail: hdkims@khu.ac.kr
***Nuclear Science and Engineering Department, Massachusetts Institute of Technology
Cambridge, MA 02139, USA
****Nuclear Reactor Laboratory, Massachusetts Institute of Technology
Cambridge, MA 02139, USA

Abstract

In recent film boiling heat transfer studies with nanofluids, it was reported that deposition of nanoparticles on a surface significantly increases the nominal minimum heat flux (MHF) or Leidenfrost Point (LFP) temperature, considerably accelerating the transient cooling of overheated objects. It was suggested that the thin nanoparticle deposition layer and the resulting changes in the physico-chemical characteristics of the hot surface, such as surface roughness height, wettability and porosity, could greatly affect quenching phenomena. In this study, a set of water-droplet LFP tests are conducted using custom-fabricated surfaces which systemically separate the effects of surface roughness height (0-15 um), wettability (0-83°) and nanoporosity (~23 nm). In addition, high-speed imaging of the evaporating droplets is used to explore the influence of these surface characteristics on the intermittent solid-liquid contacts in film boiling. The obtained results reveal that nanoporosity (not solely high surface wettability) is the crucial feature in efficiently increasing the LFP temperature by initiating heterogeneous nucleation of bubbles during short-lived solid-liquid contacts, which results in disruption of the vapor film, and that micro-posts on the surface intensify such effects by promoting intermittent liquid-surface contacts.

Key words: Leidenfrost Point, Nanoporosity, Roughness, Wettability

1. Introduction

Quenching heat transfer refers to the rapid cooling of a very hot object by immersion in a cooler liquid. The process is initially dominated by film boiling in which a continuous vapor film completely separates the liquid phase from the solid surface. During film boiling, heat transfer from the surface to the liquid takes place by conduction and radiation through the vapor layer, and thus the liquid takes a significantly longer time to evaporate than it would on a surface held at lower temperature; however, as the temperature gets closer to the *Leidenfrost point (LFP)*, intermittent and short-lived liquid-solid contacts occur at discrete locations on the surface, thus creating liquid-vapor-solid interfaces once again. Ultimately, when bubble nucleation ensues at such contact points, the vapor film is

*Received XX Xxx, 200X (No. XX-XXXX)
[DOI: 00.0000/ABCDE.2006.000000]

disrupted and the heat transfer regime transitions from film boiling to transition boiling.

In recent film boiling heat transfer studies with nanofluids, we demonstrated that deposition of nanoparticles on a surface significantly increases the nominal LFP up to ~500°C under atmospheric and saturated conditions, considerably accelerating the transient cooling of overheated objects [(1)(2)]. However, such a high LFP could not be explained by the traditional LFP models based on hydrodynamic instability of the vapor film, e.g. Berenson [(3)]'s and Henry[(4)]'s models. This suggested that the vapor film is destabilized and disrupted by a different mechanism associated with the thin nanoparticle deposition layer. Characterization of the deposition layer suggested changes in roughness, wettability, and nanoscale porosity as plausible causes for such a high LFP. Nevertheless, it was not possible to identify the exact physical mechanism of LFP enhancement because nanoparticle deposition in those experiments changed roughness height, wettability and porosity simultaneously.

In this study we investigated the *separate effects* of surface roughness, wettability and porosity on the Leidenfrost temperature of water-droplet with custom-fabricated surfaces *at the nanoscale*. This approach revealed that nanoporosity is the crucial feature in efficiently increasing the LFP temperature by initiating heterogeneous nucleation of bubbles during short-lived solid-liquid contacts, which results in disruption of the vapor film.

Nomenclature

a : capillary length (= $\sqrt{\sigma/\rho g}$)
C : adjustment coefficient
e : vapor film thickness under an evaporating droplet, m
h_{fg} : latent heat of evaporation, J/kg
k : thermal conductivity, W/m-K
P : pressure, N/m^2
R : evaporating droplet radius, m
r : nucleation cavity radius, m
T : temperature, °C, K
T_{Leid} : Leidenfrost point temperature, °C, K
T_{MHF} : minimum heat flux point temperature, °C, K
v_{fg} : specific volume, m^3/kg
μ : dynamic viscosity, kg/m-s
ρ : density, kg/m^3
σ : surface tension, N/m

Subscripts

f : liquid
g : gas
nucl : nucleation
sat : saturation

2. Experiments

2.1 Preparation of test surfaces

Surface roughness height was controlled in the range from 0 μm to 15 μm (with 5 μm increment) by fabricating cylindrical posts with 5 μm diameter on a nano-smooth silicon wafer (R_a < 0.5 nm; thickness 380 μm) (Fig. 1b). The posts were fabricated with a deep reactive-ion etching process, and were arranged on a square array of large pitch (500 μm), to prevent secondary effects, such as capillarity. The deep reactive-ion etching process to

create the posts on silicon wafer is as follow. First, a layer of Hexamethyldisilazane (HMDS) primer was deposited on a silicon wafer via a vapor deposition at 150 ºC. Then, a layer of negative photo-resist, NR71-1000P, was coated on the wafer using a spin coater spinning at 3000 rpm for 30 seconds. The HMDS helped adhesion of the negative photo-resist to the wafer. Post baking on hot plate at 150ºC for two minutes helped drying the negative photo resist. Next, the wafer was exposed under ultraviolet (UV) light of wavelength 365nm to 400 nm for 20 seconds. A mask was inserted between the UV light source and the wafer to imprint pattern of square array of 5µm circles at 500 µm pitch, where the UV light interacts with the negative photo resist. After exposure to UV, the wafer was dried again on a hot plate at 100 ºC for two minutes. The wafer was then developed in RD6 developer for 15 seconds. All the negative photoresist on the wafer, except for those that was exposed to UV light underneath the mask, was washed away by RD6 developer. The remaining patterned negative photo-resist helped protecting the wafer underneath them during reactive-ion etching, which created square array of 5 µm diameter cylindrical posts at 500 µm pitch. Subsequently, the wafer was cleaned with piranha solution to remove all negative photo-resist.

The surface intrinsic wettability was controlled by depositing a nano-smooth thin layer of gold (100 nm thick) or silicon oxide (20 nm thick) with a sputtering technique; the resulting contact angles for de-ionized water droplets were found to be 83° on the gold surface and 19° on the silicon oxide surface (see the insets of Fig. 1). Note that the presence of the micro-posts does not affect wettability (compare insets of Figs. 1a and 1b), which was expected, given the large pitch of the post array. Finally, to explore the effect of nano-porosity, we used a thin nano-porous layer (about 600 nm thick) made of silicon oxide nanoparticles (23 nm), deposited according to the layer-by-layer process described by Lee et al.[5]. The nano-porous layer further enhances in the apparent wettability (the contact angle decreases to ~0°, as shown in Fig. 1d) with respect to the smooth silicon oxide surface (19°). This is due to the well-known Wenzel effect[6]. On the other hand, the roughness height change due to the nano-porous layer is negligible (≤ 0.016 µm). In summary, using a combination of spaced-out micro-posts, and smooth and nano-porous layers we were able to control surface roughness height, wettability and nano-porosity independently. The uncertainty in contact angle measurement estimated from the repeated measurements was approximately ±1°.

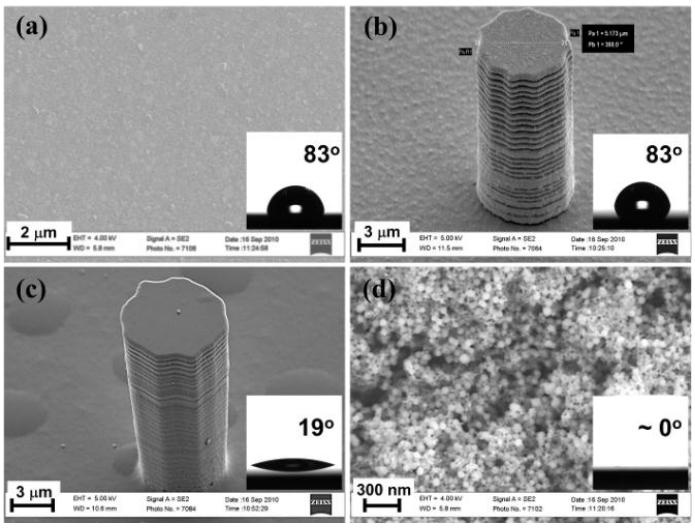

Fig. 1 SEM images of fabricated samples for LFP tests: (a) smooth Au layer; (b) 15 µm posts on smooth Au layer; (c) 15 µm posts on smooth SiO_2 layer; (d) layer-by-layer SiO_2 layer. Insets show static contact angle on the fabricated samples for 10-µL water droplets

on (a) smooth Au (83^o), (b) Au with micro-posts (83^o), (c) SiO_2 layer (19^o), (d) nano-porous SiO_2 layer (~0^o).

2.2 Measurement of LFP

A common technique used for determining the LFP consists of measuring the evaporation times of liquid droplets over a heated surface. A schematic of the experimental apparatus is shown in Fig. 2. The test surface is sandwiched between two independently heated and controlled copper blocks. The upper block has a through-hole in the shape of an inverted cone to place a droplet on the silicon wafer and keep the evaporating droplet on the silicon wafer. The temperature difference between the two blocks was controlled to be less than 1 K during the experiments. A water droplet of ~2.9 mm in diameter is released on the test surface from a height of 1.5 mm using a syringe, and the evaporation time is measured with a stopwatch. The uncertainty in the evaporation time measurement was found to be ~0.4 sec from a set of tests at representative conditions. While the nominal temperatures of the test surface measured in the copper blocks stayed within ±1 K during evaporation of a droplet, the temperature of the test surface is somewhat lower due to free convection heat loss to the ambient. This temperature drop was calculated to be less than 1.5% in the present study, relative to the total temperature difference between the copper block and the ambient. In addition, the local temperature at the location of the droplet impact is even lower due to the low heat capacity of the thin silicon plate used and the local cooling effect. The resulting nominal uncertainty in the measurement of the LFP temperature was estimated to be approximately ±5 K.

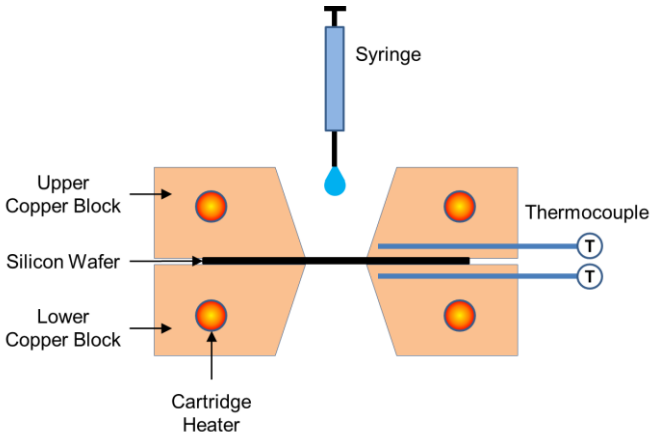

Fig. 2 Schematic of the apparatus used to measure droplet evaporation time.

3. Results

The data obtained from the droplet experiments for the surfaces without micro-posts and with the highest posts of 15 μm are displayed as droplet evaporation time vs surface temperature in Fig. 3. In this curve, the temperature corresponding to the longest evaporation time is the LFP. The LFP on the smooth gold surface without micro-posts is ~264°C, reasonably closed to the values found in the literature[7]. The LFP is slightly higher (~274°C) for the smooth silicon oxide surface without micro-posts, but is significantly higher (~359°C) for the porous silicon oxide surface without micro-posts. This result suggests that nano-porosity has a stronger effect than intrinsic surface wettability on the LFP.

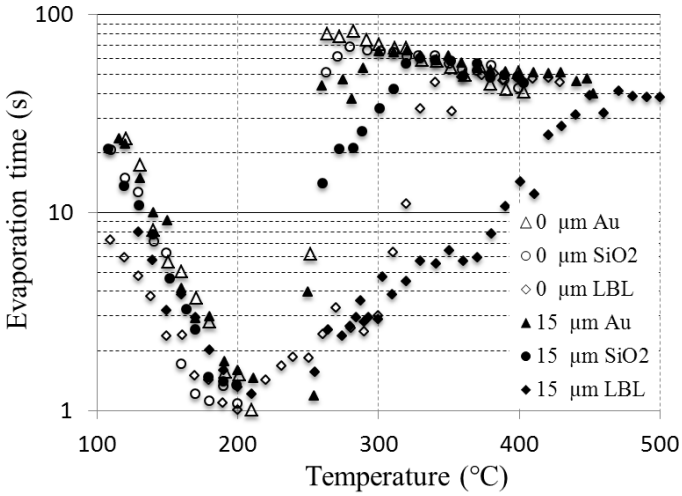

Fig. 3 Water droplet evaporation time vs. surface temperature

Figures 4-6 shows the effect of roughness height (micro-posts) respectively for the gold, silicon oxide, and porous silicon oxide surfaces. Everything else being the same, the presence of the micro-posts consistently enhances the LFP on all surfaces tested in this study, but the magnitude of the enhancement is distinctively higher on the nano-porous surface. As a result, the nano-porous surface with micro-posts can be considered an optimum (within the limits of our study), exhibiting the highest LFP at 453°C, which is even beyond the critical point of water (374°C).[1] Furthermore, it is interesting that the highest LFP on the nano-porous surface with 15-µm posts shows good agreement with the enhanced T_{MHF} (Minimum-Heat-Flux Point Temperature) measured during quenching of SiO_2 nanoparticle-coated spheres in a saturated water pool, while the nominal LFPs on the smooth Au and SiO_2 surfaces are close to T_{MHF} on the clean sphere, as shown in Figure 7. In this regard, it can be concluded that nano-porosity and micro-posts are essential features of heat transfer surfaces for such a high LFP temperature in film boiling.

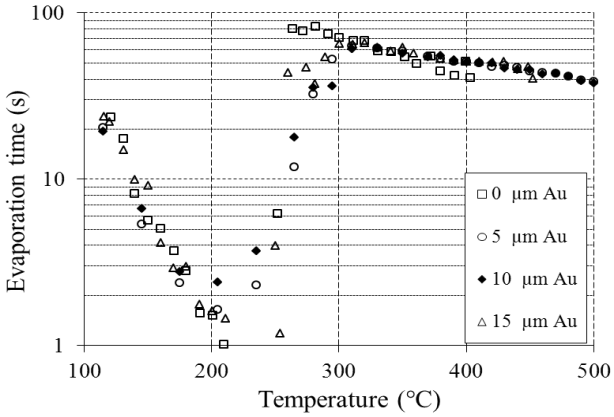

Fig. 4 Roughness effect on the LFP for gold coated surfaces

[1]Note that the reported values of LFP are the nominal temperatures of the test surface. Obviously, the local temperature at which the liquid-solid contact occurs must be below the critical point.

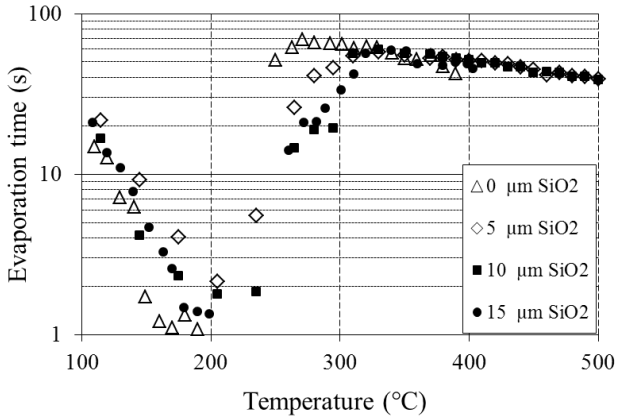

Fig. 5 Roughness effect on the LFP for silicon oxide coated surfaces

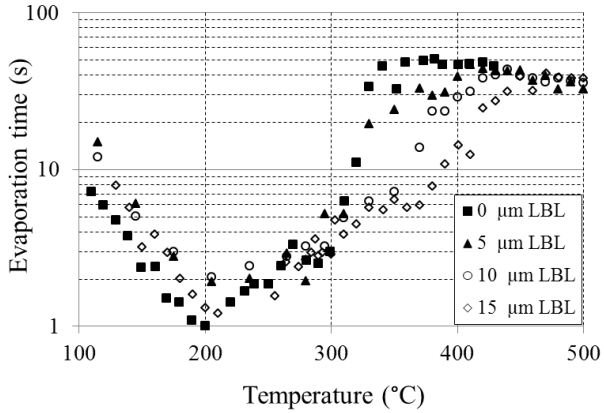

Fig. 6 Roughness effect on the LFP for SiO_2 nanoparticle layer-by-layer coated surfaces

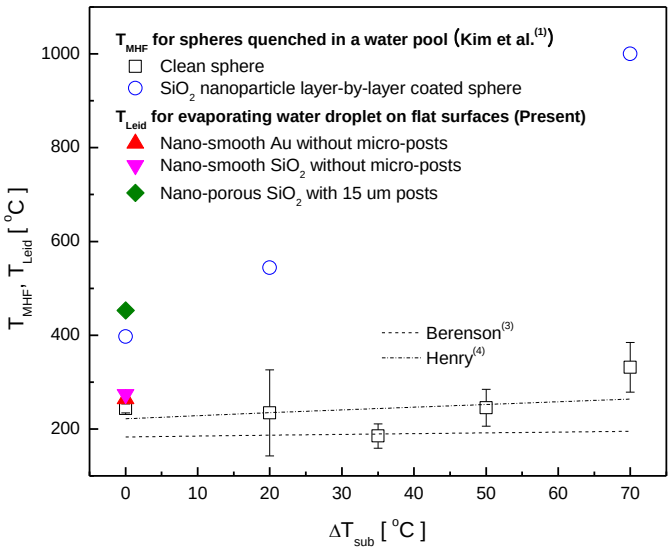

Fig. 7 Comparison of LFP for evaporating water droplet on flat surfaces and T_{MHF} for overheated spheres quenched into a water pool

4. Data Interpretation

The original motivation of this study was to identify the exact physical mechanism by which deposition of nanoparticles on a surface significantly increases the nominal LFP up to ~500°C under atmospheric and saturated conditions, considerably accelerating the transient cooling of overheated objects. The experiments presented in Section 3 have shown that heat transfer surfaces with nano-porosity and micro-posts exhibit high LFP temperature during film boiling evaporation of sessile droplets. In this section we address the key question related to the above observations: why do nano-porosity and micro-posts result in such a high LFP (Table 1)?

High-speed imaging of the evaporating droplets sheds light on the mechanisms, when we focused on the intermittent solid-liquid contacts in film boiling, as suggested by previous researches[8]. Actually, we observed thin liquid filaments intermittently connecting the droplet to the solid surface on the samples with micro-posts (Fig. 8b), whereas the filaments were not observed on the surfaces without micro-posts (Fig. 8a). However, even in the presence of liquid filaments, the evaporation process was quite different depending on whether the surface was nano-porous or not. The gold and silicon oxide surfaces without nano-porosity stably sustained the liquid filaments, typically for a few milliseconds, without triggering any perturbation (Figs. 8b and c). By contrast, the nano-porous surfaces instantaneously reacted to the filament contacts with violent splashes of tiny droplets around the large evaporating droplet (Fig. 8d). This splashing severely disturbed the liquid-vapor interface and prevented the establishment of a stable vapor film at nominal surface temperatures as high as ~453°C.

Table 1 LFP temperatures on the test surfaces (°C).

Micro post height	Au	SiO_2	Nano-porous SiO_2
0 μm	264±5	274±5	359±5
5 μm	295±5	330±5	410±5
10 μm	295±5	330±5	440±5
15 μm	290±5	325±5	453±5

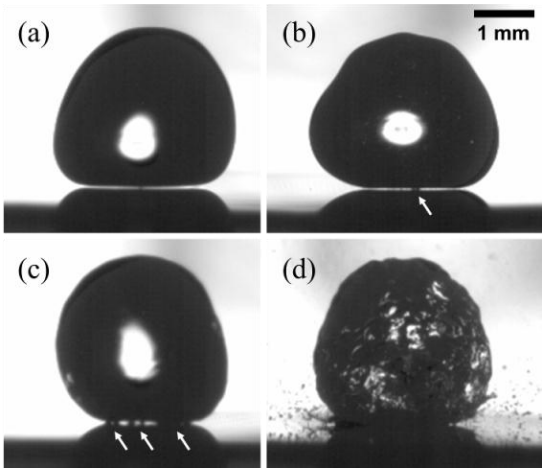

Fig. 8 Photographs of evaporating water droplets on test surfaces held at 400°C: (a) Au without posts; (b) Au with 15 μm posts; (c) SiO_2 with 15 μm posts; (d) nano-porous SiO_2 layer with 15 μm posts. Arrows show location of droplet-to-surface bridging by liquid filaments.

Biance et al.[9] derived an analytical solution for the film thickness of a stationary evaporating droplet of radius, R, smaller than the capillary length, (R<a= $\sqrt{\sigma/\rho g}$), for a

given surface superheat, ΔT,

$$e = C\left(\frac{k\Delta T\mu\rho_f g}{h_{fg}\rho_g\sigma^2}\right)^{1/3} \qquad (1)$$

where C, σ, k, μ, ρ_f, ρ_g, and h_{fg} are, respectively, an adjustable coefficient, surface tension, thermal conductivity, dynamic viscosity, density of liquid, density of vapor, and latent heat of evaporation. For an evaporating droplet of 2R ~ 2.9 mm on a surface of 400°C (ΔT=300°C), the initial film thickness is estimated to be approximately 36 μm and then decreases monotonically as $R^{4/3}$. Thus, at 15-μm height, the micro-posts can initiate solid-liquid contacts, as shown in Fig. 8.

Once the liquid filaments are established, heterogeneous nucleation of bubbles can occur at the contact points, if there are cavities available for nucleation. Bernardin and Mudawar[10]'s heterogeneous nucleation model of the LFP focuses on the surface superheat temperature required to initiate the growth of hemispherical vapor bubbles from the pre-existing surface cavities. The nano-sized pores act as cavities for heterogeneous nucleation of bubbles. The pressure drop across a spherical bubble interface of radius r can be estimated using Young-Laplace equation as

$$P_g - P_f = 2\sigma/r \qquad (2)$$

In combination with the Clausius-Clapeyron equation, Eq. (2) gives the following expression for the temperature required to initiate the nucleation of a hemispherical vapor bubble[10],

$$T_{nucl} = T_{sat}\exp\left(\frac{2\sigma v_{fg}}{rh_{fg}}\right). \qquad (3)$$

There exists a large difference in temperature for heterogeneous nucleation of bubbles between the nano-porous and non-porous surfaces, i.e. $T_{nano\text{-}porous}$ ~ 218°C versus $T_{non\text{-}porous}$ ~ 336°C, where nucleation diameter of 23 nm and 1 nm were assumed, respectively. Therefore, bubbles more easily nucleate on the nano-porous surface and very rapidly grow in the highly superheated liquid. Note that these values of nucleation superheat are much higher than those normally encountered on engineering surfaces where micro-cavities are present. The calculated value of the heterogeneous nucleation temperature at d = 1 nm is higher than the homogeneous nucleation temperature (~300°C for water at atmospheric pressure) because the size of the vapor embryos responsible for homogeneous nucleation is of the order of a few nm. Therefore, the fluid nucleates homogeneously before it does so heterogeneously.

Starting from the Rayleigh equation for the inertia-controlled phase of bubble growth, it can be shown that $\Delta P \sim \rho V^2$, where V is the velocity of the expanding vapor interface and ΔP is the value of the pressure difference across the interface at the point of nucleation. For a bubble with a diameter of 23 nm, the estimated velocity, V, is of the order of 10 m/sec. When the vapor phase velocity is greater than the critical velocity of Kelvin-Helmholtz instability, the liquid-vapor interface can be disrupted. For the steam and water at atmospheric pressure, the critical velocity is approximately 8 m/sec[11]. Therefore the velocity of the expanding vapor interface for the 23 nm-diameter bubble is fast enough to generate the splashes shown in Fig. 8d.

The insights obtained in the present study allow us to describe the physical mechanism associated with some interesting observations in previous studies: deposition of

nanoparticles on a surface significantly increases the nominal minimum heat flux (MHF) or Leidenfrost Point (LFP) temperature[1], and the propagation velocity of the quench front can be significantly enhanced, from order of mm/s to order of m/s, due to the nanoparticle deposition on the surface of metallic rodlets[2]. Initially, micro-sized structures (such as posts) promote intermittent solid-liquid contacts in film boiling at a high temperature; if the surface has nano-pores , vigorous nucleation of bubbles ensues and results in strong splashes locally destabilizing the vapor film. Such splashes have high velocity of the order of m/sec, thus causing so secondary liquid/solid contacts along the surface. As a result, the entire vapor film around the quenched objects can be effectively destabilized and disrupted very fast, even at very high temperatures.

4. Conclusions

Water-droplet Leidenfrost Point (LFP) tests were carried out using custom-fabricated surfaces which separate the effects of surface roughness, wettability and porosity. The findings from the results are as follows:

- Nano-porosity (not solely high surface wettability) is an essential feature to enhance the LFP, and such enhancement occurs via prevention of the stable vapor film establishment, caused by heterogeneous nucleation of bubbles;

- Micro-posts on the surface intensify such effects by promoting intermittent liquid-surface contacts.

The heat capacity of the silicon plate used in this study was small. Some researchers, for example, Baumeister and Simon[12], reported that heat capacity has a strong effect on LFP temperature. Therefore, the results obtained in the present experiments apply in the limit of small heat capacity. Additional work is needed to extend the conclusions of this study to the case of any surface heat capacity.

5. Acknowledgements

This work was supported by the Korea Science and Engineering Foundation (KOSEF) grant funded by the Korea government (MEST) (No. 2010-0018761). The authors acknowledge the financial support of the DOE-NEUP fellowship program for Dr. Bao Truong. We also thank Mr. Eric Forrest for assisting in the preparation of the layer-by-layer coatings of the test samples in Profs. M. Rubner and R. Cohen's lab at MIT.

6. References

(1) H. Kim, G. DeWitt, T. McKrell, J. Buongiorno, and L.-W. Hu, "On the quenching of steel and zircaloy spheres in water-based nanofluids with alumina, silica and diamond nanoparticles", Int. J. Multiphase Flow, Vol. 35(5), 2009, pp. 427-438.
(2) H. Kim, J. Buongiorno, L.-W. Hu, T. McKrell, " Nanoparticle deposition effects on the minimum heat flux point and quench front speed during quenching of rodlets and spheres in water-based alumina nanofluids", Int. J. Heat Mass Transfer, Vol. 53, 2010, pp. 1542-1553.
(3) P. L. Berenson, "Film-boiling heat transfer from a horizontal surface", J. Heat Transfer, Vol. 83, 1961, pp. 351-358.
(4) R. E. Henry, "A correlation for the minimum film boiling temperature", AlChE Symp. Ser. , Vol. 70, No. 138, 1974, pp. 81-90.
(5) D. Lee, M. F. Rubner, and R. E. Cohen, "All-nanoparticle thin-film coatings", Nano Letters,

Vol. 6, No. 10, 2006, pp. 2305-2312.
(6) R. N. Wenzel, “Resistance of solid surfaces to wetting by water”, Ind. Eng. Chem., Vol. 28, No. 8, 1936, pp. 988-994.
(7) S. C. Yao and K. Y. Cai, “The dynamics and Leidenfrost temperature of drops impacting on a hot surface at small angles”, Exp. Therm. Fluid Sci. , Vol. 1, 1988, pp. 361–371.
(8) W. S. Bradfield, “Liquid-solid contact in stable film boiling”, Ind. Eng. Chem. Fundamen. , Vol. 5, No. 2, 1966, pp. 200-204.
(9) A.-L. Biance, C. Clanet, and D. Quere, “Leidenfrost drops”, Phys. Fluids, Vol. 15, No. 6, 2003, pp. 1632-1637.
(10) J. D. Bernardin and I. Mudawar, “A Cavity Activation and Bubble Growth Model of the Leidenfrost Point”, J. Heat Transfer, Vol. 124, 2002, pp. 864-874.
(11) Van P. Carey, Liquid-Vapor Phase-Change Phenomena, 2nd ed., Taylor & Francis, New York, 2008, pp. 112-121.
(12) K. J. Baumeister and F. F. Simon, “Leidenfrost Temperature - Its correlation for liquid metals, cryogens, hydrocarbons, and water”, ASME Journal of Heat Transfer, Vol. 95, 1973, pp. 166-173.